FISEVIER

Contents lists available at ScienceDirect

Journal of Colloid And Interface Science

journal homepage: www.elsevier.com/locate/jcis

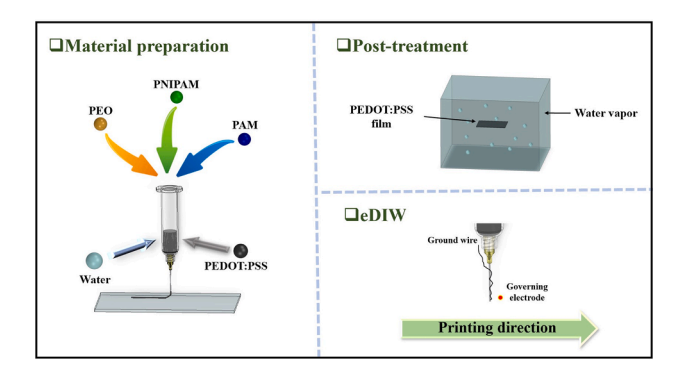




Extremely-fast electrostatically-assisted direct ink writing of 2D, 2.5D and 3D functional traces of conducting polymer Poly (3,4-ethylenedioxythiophene) polystyrene sulfonate- polyethylene oxide (PEDOT:PSS-PEO)

J. Plog ^{a,1}, X. Wang ^{a,1}, K.M. Lichade ^a, Y. Pan ^{a,*}, A.L. Yarin ^{a,b,*}

GRAPHICAL ABSTRACT



ARTICLE INFO

Keywords: PEDOT:PSS Secondary doping Humidity Direct Ink Writing

ABSTRACT

Hypothesis: Poly(3,4-ethylenedioxythiophene)-poly(styrenesulfonate) (PEDOT:PSS) is an attractive conducting polymer, albeit its rheological properties are inappropriate for direct ink writing (DIW). Here it is hypothesized that a suspension of PEDOT:PSS with a non-conducting highly spinnable viscoelastic polymer, e.g., polyethylene oxide (PEO), will significantly facilitate printability and enhance the electrical conductivity (EC) of PEDOT:PSS-PEO. It is also hypothesized that high-humidity post-treatment will enhance the EC even further, and the application of the electric field can facilitate the DIW speed beyond the capabilities of current commercial 3D printers.

Experiments: The rheological behavior of PEDOT:PSS suspensions with several non-conducting polymers was explored in the experiments. The EC of the suspensions was measured, including the effect of high-humidity post-treatment. High-speed DIW of the optimal suspension was experimentally demonstrated with the applied electric field.

a Department of Mechanical and Industrial Engineering, University of Illinois at Chicago, 842 W. Taylor St, Chicago, IL 60607-7022, USA

^b School of Mechanical Engineering, Korea University, Seoul 136-713, Republic of Korea

^{*} Corresponding authors.

E-mail addresses: yayuepan@uic.edu (Y. Pan), ayarin@uic.edu (A.L. Yarin).

 $^{^{1}}$ Contributions: J. Plog and X. Wang contributed equally to this work.

Findings: The findings revealed that PEO serves as a secondary dopant, and the suspension of 4.33 wt% PEDOT: PSS-52 wt% PEO possesses the EC > 15 times higher than that of PEDOT:PSS. Many 2D, 2.5D and 3D functional traces were printed at high resolution at the DIW speed up to 8.64 m/s (>10 times faster than current commercial printers), facilitated by the applied electric field. Post-treatment at 80–90% relative humidity enhanced the EC more than twice.

1. Introduction

Conducting polymers (CPs) or, more accurately, intrinsically conducting polymers (ICPs), possess unique electrical, optoelectronic, and mechanical properties [1-4]. Since H. Shirakawa, A. Heeger, and A. MacDiarmid discovered the first CP in 1977 [5-7], the field of CPs has grown exponentially in the past few decades. With>25 polymers belonging to the class [8], the most common CPs include polyacetylene, poly(3,4polyaniline, polypyrrole, polythiophene, and ethylenedioxythiophene):poly(styrene sulfonate) (PEDOT:PSS) [9-12]. Recently, PEDOT:PSS has dominated literature due to its remarkable chemical stability, good film-forming properties, moderate stretchability, and water dispersibility. These attributes have elevated PEDOT: PSS to become one of the most successful conducting polymers in today's industry [13-16]. Most common commercial PEDOT:PSS suspensions that contain 1 wt% PEDOT:PSS are low-viscosity and highly rely on conventional manufacturing methods, such as spin coating [17], dip coating [18], and inkjet printing [19]. Recently, these manufacturing processes have already been applied to fabricate a variety of electronic devices, including biosensors, electrodes, organic electronic ion pumps, solar energy conversion devices, and rechargeable batteries [20-24]. However, the above manufacturing processes limit the application of the PEDOT:PSS-based material to a one-dimensional or two-dimensional structure, which reduces the design novelty and hinders its application.

Additive manufacturing (AM) techniques, also known as 3D printing, have been highly instrumental in driving technological advances in recent years. AM holds great promise for fabricating complex 2.5D and 3D structures compared to traditional manufacturing processes. Direct ink writing (DIW) is an extrusion-based AM method highlighted by its excellent ability to print complex 2.5D and 3D designs using various materials, including ceramics, polymers, metals, and composites [25]. In DIW, the pressure inside the printing nozzle is controlled to dispense functional ink onto a substrate according to the predefined paths, allowing a model to be built in a layer-by-layer fashion. An ideal DIW printable ink should possess appropriate shear-thinning properties, thixotropy, and viscoelasticity [26]. These three types of rheological behavior enable ink to be smoothly and continuously extruded from the nozzle while retaining its shape after the extrusion [27]. With these attributes, DIW addresses fundamental problems that plague traditional manufacturing when attempting to produce materials or objects for applications in flexible electronics, smart textiles, or soft robotics. It should be emphasized, however, that the commercial PEDOT:PSS is not suitable for DIW processes due to its low viscosity.

A few studies focused on altering the rheological properties of commercial aqueous PEDOT:PSS suspensions. It was demonstrated that concentrations of PEDOT:PSS nanoparticles in water in the 5 to 7 wt% range result in acceptable shear-thinning and viscoelastic characteristics. In other words, the ideal rheological properties needed for printability in DIW were seemingly achieved [28]. However, the downside of this approach is the complex steps required to prepare the ink.

Furthermore, the commercial PEDOT:PSS suspensions have very low electrical conductivity (EC), which makes them unsuitable for electronic devices. Researchers investigated various methods to enhance the electrical conductivity of PEDOT:PSS. One well-known method is to use the organic solvent treatment. With significant dipole moments (being polar), these fluids combine readily with the aqueous PEDOT:PSS suspensions. Numerous solvents beneficial to PEDOT:PSS film conductivity

were found, in particular, highlighting dimethylformamide (DMF), tetrahydrofuran (THF) and dimethyl sulfoxide (DMSO) yielding gains from 0.8 to 80 S cm⁻¹ [29]. Treatments with polar organic solvents have yielded yet another factor of ten when using ethylene glycol (EG) [30], sorbitol [31], and glycerol [32]. While promising for several traditional manufacturing techniques, adding polar organic solvents to PEDOT:PSS is not working for making DIW inks because their relatively high boiling points make it difficult to solidify the extruded ink. Since DIW builds objects layer by layer, the high boiling points of the added solvents would dramatically increase the drying time to unacceptable intervals between layer-to-layer deposition.

In this work, first, we demonstrate the development of DIW-printable viscoelastic PEDOT:PSS-based inks starting from a commercial aqueous suspension with the addition of a second polymer working as a dopant [33]. Three secondary polymers, PEO, PNIPAM, and PAM, were added at different concentrations, and the resulting electrical conductivities and rheological properties were characterized. Next, we present an effective strategy to create an ideal PEDOT:PSS-based DIW suspension by hydrating dry pellets at different concentrations. While this method drastically increases the EC and printability of PEDOT:PSS-based aqueous suspensions compared to those commercially available, further improvements were revealed using PEO as a secondary dopant. The addition of the secondary polymer PEO not only makes the inks more DIW-friendly, but also results in a non-trivial enhancement in the EC. After testing different concentrations of PEO, the ink formulation was optimized and used to print three-dimensional PEDOT:PSS structures using the DIW process. Finally, samples were also printed using an electrostatically-assisted direct ink writing (eDIW) process, which was developed by the present group to increase printing speed and resolution while simultaneously decreasing defects [34]. After printing, some eDIW-printed specimens were post-processed in humidity-controlled environments and the electrical conductivity was measured again, showing an additional significant enhancement.

2. Materials and methods

2.1. Materials

Modified commercial PEDOT:PSS aqueous suspension.

A PEDOT:PSS aqueous suspension (1 wt% PEDOT:PSS in the suspension) was purchased from Heraeus (Hanau, Germany) and used as a base to add the thickening (and simultaneously doping) polymers. The base PEDOT:PSS suspension was stirred at room temperature for three hours to eliminate any aggregates. The PEDOT:PSS suspension was then divided into four equal portions, each containing 5 g of the suspension. To increase the shear viscosity and viscoelasticity of the base PEDOT: PSS, secondary dopants including polyethylene oxide (PEO) ($M_v=100\,$ kDa, Sigma-Aldrich, St. Louis, MO) poly(N-isopropylacrylamide) (PNI-PAM) ($M_w=300\,$ kDa, Scientific Polymer Products Inc. Ontario, NY), and polyacrylamide (PAM) ($M_w=5000\,$ kDa, Sigma-Aldrich, St. Louis, MO) were added to the PEDOT:PSS suspension, separately. The blends were subsequently magnetically stirred for 17 h at room temperature to ensure the preparation of homogeneous and stable blend suspensions.

The experimental results demonstrated that when the weight ratio of PEO (defined as the ratio of the PEO solid in the total weight of all solids: the PEO solid weight/(the PEO solid weight + PEDOT:PSS solid weight)) reached the value of 95.34 wt%, the PEDOT:PSS/PEO aqueous suspension revealed sufficient viscoelasticity for printing. When the weight

ratios of PNIPAM and PAM reached the values of 77.78 wt% and 86.84 wt%, respectively, the resulting PEDOT:PSS/PNIPAM aqueous suspension and PEDOT:PSS/PAM aqueous suspension revealed sufficient viscoelasticity for printing. The three formulations are denoted as PEDOT:PSS-95.34 wt% PEO, PEDOT:PSS-77.78 wt% PNIPAM, and PEDOT:PSS-86.84 wt% PAM in the following discussions. Their rheological properties are tested and plotted in Fig. 2, and discussed in section 3.1.

Suspensions of modified dry re-dispersible PEDOT:PSS pellets.

The second method used for preparing the suspension involved the use of dry re-dispersible PEDOT:PSS pellets along with PEO as a dopant. The PEDOT:PSS pellets obtained from Sigma-Aldrich (St. Louis, MO) were mixed with deionized (DI) water in concentrations of 1 wt%, 2.5 wt %, and 4.33 wt% (i.e., the weight ratio of PEDOT:PSS in the aqueous suspension after the pellets are completely dispersed), respectively. To ensure a homogeneous PEDOT:PSS aqueous suspension, the mixtures were stirred at room temperature for one day. The resulting three inks are named as 1 wt% PEDOT:PSS, 2.5 wt% PEDOT:PSS, and 4.33 wt% PEDOT:PSS. Their rheological properties are tested and plotted in Fig. 3, and discussed in section 3.2.

In addition, to further test the effects of secondary dopants on the printability and electrical conductivity, two additional inks were prepared by adding 52 wt% of PEO [i.e., PEO weight ratio is defined as: PEO solid weight/(PEO solid weight + PEDOT:PSS solid weight)] into the 2.5 wt% PEDOT:PSS suspension and 52 wt% of PEO into the 4.33 wt% PEDOT:PSS suspension. To achieve stable and homogeneous blend suspensions, after adding PEO solids, the blends were stirred for 24 h. The resulting two homogeneous suspension inks are named as 2.5 wt% PEDOT:PSS-52 wt% PEO and 4.33 wt% PEDOT:PSS-52 wt% PEO in the following discussions. Their rheological properties are tested and plotted in Fig. 3 and discussed in section 3.2.

2.2. Methods

Measurements of flow curves in simple shear flow.

The shear viscosity and shear stress of the blended inks was measured using a rotational rheometer (Kinexus Ultra+, NETZSCH Instruments, Burlington, MA). The gap distance between the two parallel plates in the simple shear experiments was 0.2 mm, and the room temperature was monitored throughout the experiments without significant fluctuations.

Measurements of thixotropy.

In this study, the thixotropic properties of the materials were measured using the 3 Interval Thixotropy Test (3-ITT), to investigate the rheological behavior of inks during the DIW printing process. The rheometer, distance between parallel plates, and temperature were identical to those described in the previous section. The testing procedures were as follows. First, the material was sheared for 60 s at 1 s⁻¹. The shear rate was then increased to $100 \, {\rm s}^{-1}$ for a duration of 30 s. The shear rate was subsequently reduced to $1 \, {\rm s}^{-1}$ for 150 s. The recovery performance can be calculated by the following equation [35]

$$R = \frac{\eta_1}{\eta_0} \times 100\% \tag{1}$$

where η_0 is the initial viscosity of the material; η_1 is the recovery viscosity of the material; R represents the recovery degree.

Measurements of viscoelastic properties in uniaxial elongation flow. The viscoelastic characteristics were measured using an elongational viscometer based on self-thinning capillary thread. The method is described in detail in the following publications: [36–41]. In brief, the viscoelastic thread diameter d decreases in time t due to capillary squeezing starting from an initial value $d=d_0$ at t=0. If the decrease is exponential in time, the tested liquid is viscoelastic. Then, the slope $-1/(3\theta)$ of the dependence of $\ln(d/d_0)$ on t is used to measure the viscoelastic relaxation time θ .

DIW: 3D printing procedure for thin film.

In this study, a dispensing robot (E3V, Nordson EFD), an extrusion pressure pumping system (Ultimus II, Nordson EFD), and a stainless-steel dispensing nozzle (0.6 mm inner diameter) were integrated to develop the DIW system. Thin films were printed using the DIW system to measure the electrical conductivity (EC). The standoff distance between the dispensing nozzle and the substrate was adjusted to 0.25 mm. The platform temperature was increased to 60 $^{\circ}$ C for 30 min to facilitate the solidification of the printed thin films. Additionally, a high-speed camera (Phantom VEO-E 340L) equipped with back-light shadow-graphy was used to capture the extrusion process in the DIW system.

Electrical conductivity measurement.

The DIW printer was utilized to print the 20 mm \times 20 mm thin films on glass slides using conducting PEDOT:PSS-based inks developed as described in section 2.1. After solidification, a 4-point probe (Veeco FPP-100) measured the electrical conductivity of the films. This commercial measuring device uses four equally spaced probes centered and pressed onto the conducting films with repeatable force.

A Keithley 2400 SourceMeter applied current to the outer probes, and the voltage was measured on the inner two probes using Fluke 8845 precision multimeter. Specimens for each ink composition were grouped and tested twice at slightly different locations near the film center. The following equation was used to calculate the sheet resistances [42]

$$R_s = \frac{\pi}{\ln(2)} \frac{\Delta V}{I} \tag{2}$$

where R_S is the sheet resistance, ΔV is the voltage measured by the multimeter, and I is the current measured by the ammeter. A surface profiler measured the film thickness h. Then, the electrical conductivity S was found from the following equation

$$S = \frac{1}{R_c h} \tag{3}$$

A novel setup for electrostatically-assisted direct ink writing (eDIW), as shown in Fig. 1, employs an additional electrostatic force to pull the ink jet in the printing direction after extrusion. The 22-gauge printing needle is directly grounded to a high-voltage power, which applies a positive potential to the governing electrode. This electrode is positioned adjacent to the printing needle near its exit and always pulls the ink in the opposite direction of the substrate motion, as recently demonstrated by the present group in Refs. [33,43].

Humidity post-treatment in humidity chamber.

After drying at 60 °C, the EC and thickness of the specimens were measured before placing into a humidity-controlled environment. Five individual chambers were held at 75, 80, 85, 90, and 99% relative humidity using a proportional integral derivative in-house (PID) program, Arduino Uno microcontroller, relays (5 V Relay Module), air solenoids (Mini Electric Solenoid Valve), fogger (Ultrasonic Atomizer Air Humidifier), and humidity sensors (DHT11). For the control specimens, an additional slotted chamber was vented to the laboratory with the humidity being monitored. This setup maintained the relative humidity levels within a \pm 1% relative to the set point. Each chamber was monitored and functioned independently of the other units. This humidity post-treatment was conducted for 4 h before specimen drying and the second EC measurement.

DIW-3D printing procedure of three-dimensional structures.

Specimens were printed on glass slides by a commercial dispensing robot (E3V, Nordson EFD) at a speed of 0.03 m/s using a 22-gauge needle. A heating plate set to 70 $^{\circ}\mathrm{C}$ was used to facilitate rapid water evaporation from within the structure.

3. Results and discussion

Here, we aim to modify commercial PEDOT:PSS aqueous suspensions to improve their rheological characteristics for higher DIW

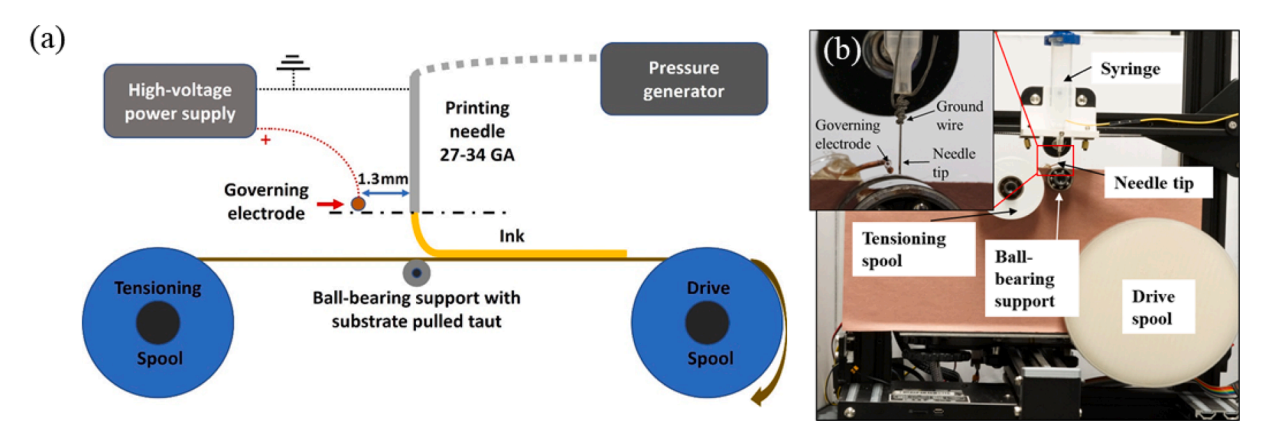


Fig. 1. The eDIW setup. (a) Schematic of the experimental setup. (b) The eDIW prototype.

printability while maintaining or enhancing the EC of prints. In a previous study of the present group [33], which aimed to refine DIW prints, the pristine aqueous PEDOT:PSS ink was doped with secondary polymers including PEO and PNIPAM with varying weight ratios. The rheology of these blends were characterized in [33]. It was found that with a higher weight ratio of the secondary polymer (i.e., PEO, or PNIPAM), the PEDOT:PSS-based blends revealed a higher viscosity and higher printability in DIW. Samples were printed with the prepared inks and their electrical conductivities (EC) were characterized. In contrast to PNIPAM, PEO (at concentrations below 52 wt%) was found to increase the EC above that of pristine PEDOT:PSS. The most significant gain in the EC of PEDOT:PSS-PEO prints was observed at 52 wt% of PEO. Increasing PEO concentration beyond 52 wt% decreased the EC of printed thin films of PEDOT:PSS-PEO [33,44]. The following sections describe a further modification of pristine commercial PEDOT:PSS aqueous suspensions in the present work. Note that specific details of procedures are given in section 2.

${\it 3.1.} \ {\it Rheological behavior of modified commercial PEDOT:PSS aqueous suspension}$

PEDOT:PSS aqueous suspensions (12 nm-19 nm in diameter [45]) were blended with additional (doping) polymers, forming homogeneous inks. Then, the rheological properties of these inks were characterized in shear, thixotropy, and uniaxial elongation, to investigate their printability, viscosity recovery, and freeform shape-retention capability. It is crucial to ensure that any improvements made to printability do not compromise the electrical conductivity (EC). Fig. 2 (a) and 2(b) illustrate the flow curves and viscosities of pure aqueous solutions of additional polymers at the same concentrations as those added to the PEDOT:PSS suspensions, measured at a shear rate of 1 s⁻¹. Pure PNIPAM and PEO solutions were less viscous than PEDOT:PSS containing PNI-PAM or PEO [Fig. 2(e)]. One possible explanation is that PEO/PNIPAM weakens the attractive force between PEDOT and PSS, allowing the short PEDOT chains to interconnect and form long PEDOT chains [46,47]. Long chains can easily entangle and form a network that increases the shear viscosity of the material. In addition, the viscosity of the pure PAM solution is identical to the viscosity of PEDOT:PSS with PAM, indicating that the PAM solution was the primary factor in improving the viscosity of the materials. The measured shear viscosities of blends (the flow curves) are presented in Fig. 2(c), with procedural details combined in sections 2.1 and 2.2. Similarly to our previous study [33], the PEDOT:PSS inks demonstrated shear-thinning behavior. As the shear rate increases, the shear viscosity reduced. A potential reason might be the long polymer coils stretching and aligning in the flow direction. Fig. 2(d) demonstrates that as the shear rate increased, the slope of the shear stress versus the shear rate curve decreased, also indicating that PEDOT:PSS with a high weight ratio of PEO, PNIPAM, and PAM

exhibited shear-thinning properties. It should be emphasized that in the range of the shear rates explored in the present work, none of the polymer solutions revealed any traces of the existence of a yield stress, i. e., none of them demonstrated any features characteristic of the Bingham fluids. Fig. 2(e) reveals that PEDOT:PSS with a high-weight percentage, as well as PEO, PNIPAM, and PAM, exhibit high viscosity at low shear rates of approximately 1 s⁻¹. This characteristic is advantageous in preventing the print from spreading on the substrate before solidification occurs via solvent evaporation. Such shape retention capabilities offer great potential for printing freeform structures that maintain their shape after deposition, without collapsing. The 3-ITT results shown in Fig. 2(f) indicated that PEDOT:PSS with a high ratio of additional doping exhibits thixotropic behavior in the third interval. All the materials were capable of regaining their viscosity after extrusion, which allows the ink to retain its shape after extrusion. PEDOT:PSS with PEO and PAM had the highest recovery degree, which was nearly 100%. PEDOT:PSS with PNIPAM demonstrated a recovery degree of 84.62%.

3.2. Rheological behavior of modified dry re-dispersible PEDOT:PSS

The shear viscosity of all the materials decreased as the shear rate increased, as shown in Fig. 3 (a). The slope of the shear stress versus the shear rate decreased as the shear rate increased, as depicted in Fig. 3(b). These two results indicated that these materials exhibit shear-thinning behavior. Besides, the results in Fig. 3(a) and 3(b) reveal that a higher concentration of the initially dry PEDOT:PSS nanoparticles suspended in water significantly increases the shear viscosity at any shear rate. At the same time, adding PEO at the optimum ratio of 52 wt% [33,44] had a less pronounced effect on the shear viscosity [cf. Fig. 3(a)], which indicates the effectiveness of the PEO addition in increasing the ink printability.

In addition to the behavior in the simple shear flows, rheological behavior in the uniaxial elongation flows is important for the polymer suspension inks to be extruded successfully during the DIW process. Accordingly, capillary thinning of thin polymer solution threads was used as an elongational rheometer here; cf. section 2.2. Fig. 3(c) and 3(d) plot the diameter of the filament versus time for the 2.5 wt% PEDOT: PSS-52 wt% PEO and the 4.33 wt% PEDOT:PSS-52 wt% PEO suspensions, respectively. The ink naming protocols were explained in section 2. For example, for the ink named 2.5 wt% PEDOT:PSS-52 wt% PEO, the PEDOT:PSS weight versus the total weight of PEDOT:PSS solid and water is 2.5%, and the PEO solid weight versus the total weight of PEDOT:PSS solid and the PEO solid is 52%. The suspension threads employed in these measurements are detailed in section 2.2. The lowerconcentration suspension reveals a non-exponential decrease of the thread diameter with time in Fig. 3(c), which is characteristic of either viscous Newtonian, or power-law fluids [40]. Indeed, the dependence d = d(t) which is not of the type of $d/d_0 = \exp(-t/3\theta)$, was previously

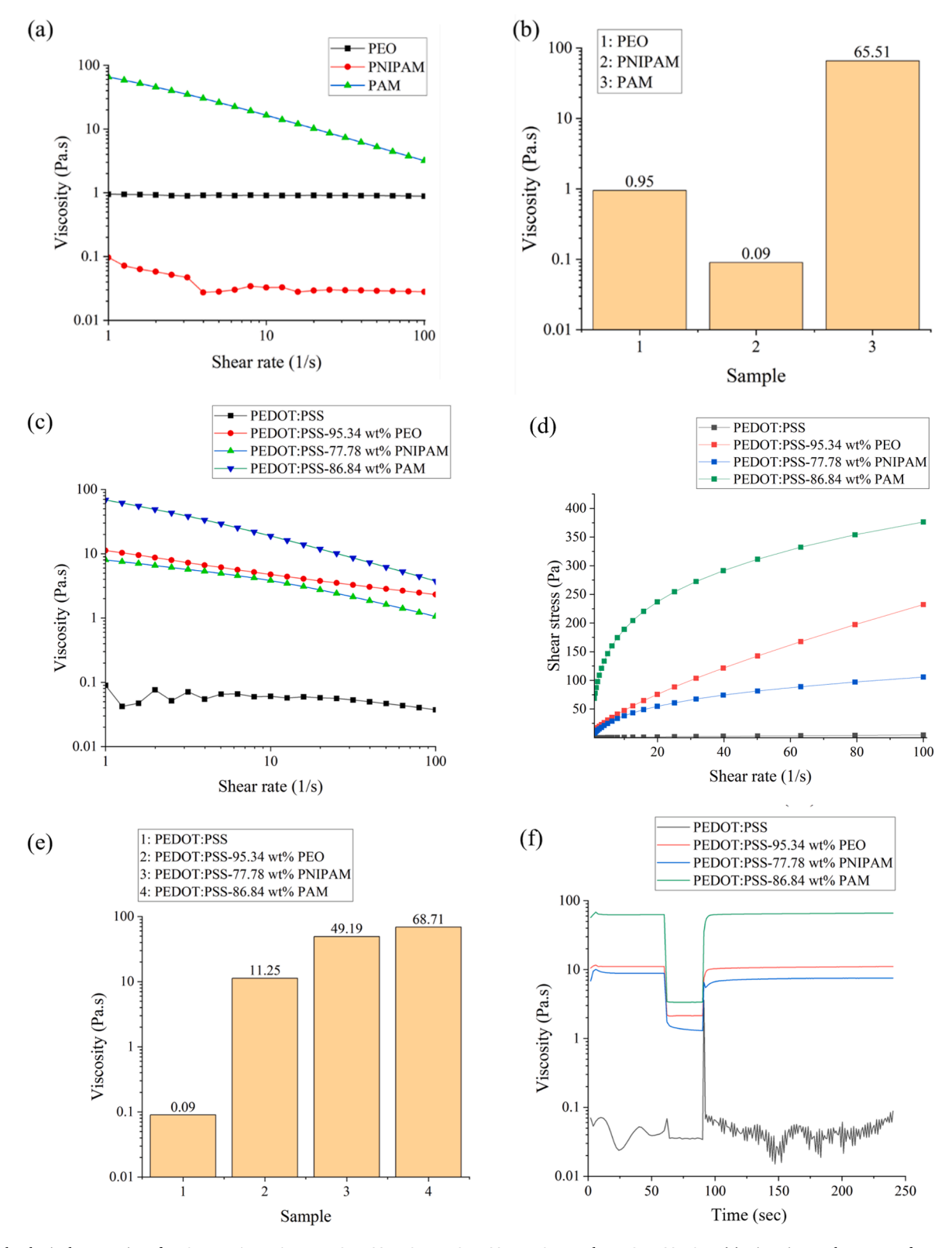
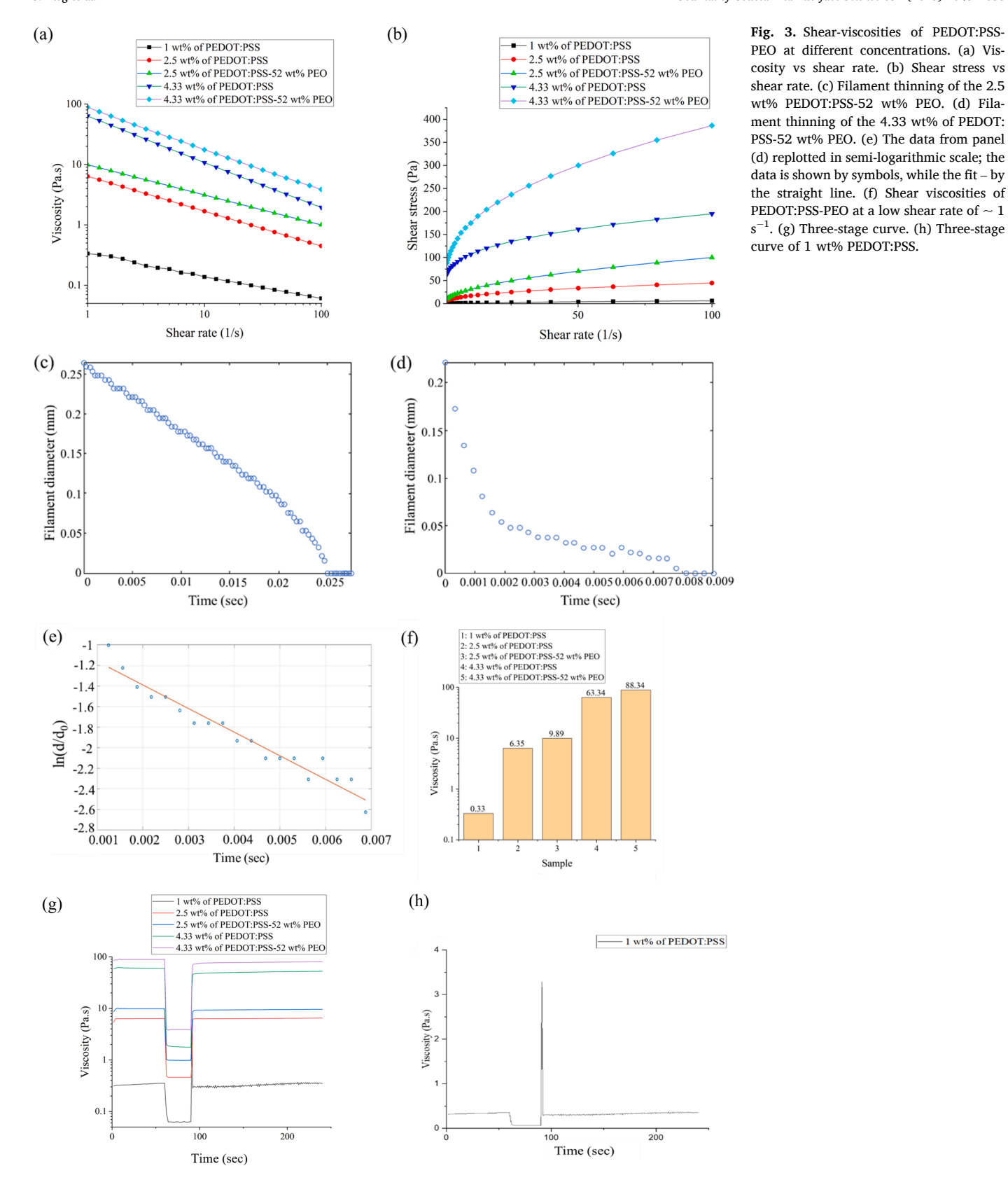


Fig. 2. Rheological properties of PEO, PNIPAM, PAM, PEDOT:PSS-PEO, PEDOT:PSS-PNIPAM, and PEDOT:PSS-PAM. (a) Viscosity vs shear rate of pure additional doping solutions. (b) Shear viscosities at the shear rate of 1 s⁻¹ of pure additional polymer solutions. (c) Viscosity vs shear rate of PEDOT:PSS-PNIPAM, and PEDOT:PSS-PAM. (d) Shear stress vs shear rate of PEDOT:PSS-PEO, PEDOT:PSS-PNIPAM, and PEDOT:PSS-PAM. (e) Shear viscosities of PEDOT:PSS-PEO, PEDOT:PSS-PNIPAM, and PEDOT:PSS-PNIPAM, and PEDOT:PSS-PAM. at a low shear rate of $\sim 1 \text{ s}^{-1}$. (f) Three-stage curve of PEDOT:PSS-PEO, PEDOT:PSS-PNIPAM, and PEDOT:PSS-PNIPAM, and PEDOT:PSS-PAM.



observed for Newtonian or the Ostwald-de Waele power-law types of non-Newtonian fluids [40]. On the other hand, the exponential decrease in the thread diameter in time in Fig. 3(d) and 3(e) corresponds to the $d/d_0=\exp(-t/3\theta)$ type [36–39,41] and allows one to measure the relaxation time of $\theta=0.0015$ s, which is the most important rheological

parameter characterizing viscoelasticity. One can conclude that of the two suspensions explored, only the higher-polymer concentration 4.33 wt% PEDOT:PSS-52 wt% PEO suspension is viscoelastic.

Furthermore, 3-ITT results [Fig. 3(g)] revealed that all the materials had thixotropic properties in the third interval. When the shear rate

decreased from $100~s^{-1}$ to $1~s^{-1}$, the viscosity of 1 wt% PEDOT:PSS revealed a sharp rise, then abruptly dropped to its initial value [cf. Fig. 3 (h)]. The recovery degrees of 1 wt% PEDOT:PSS and 2.5 wt% PEDOT: PSS were nearly 100%. The recovery degree of 4.33 wt% PEDOT:PSS material was 87.95%. After adding 52 wt% of PEO, the recovery degree increased to 90.12%.

At a dispersion concentration of 4.33 wt% PEDOT:PSS, with 52 wt% PEO added (when dried), the modified PEDOT:PSS (re-dispersed pellets) suspensions were transformed into a 3D-printable gel with both shearthinning and viscoelastic properties. As shown in Fig. 4, the printed filament exhibited optimal extrusion behavior and excellent shape retention.

3.3. Electrical conductivity in thin DIW-printed films

DIW was used to repeatedly print thin films using a procedure described in section 2.2. The results revealed that adding doping polymer at high loading fractions to a commercial PEDOT:PSS aqueous suspension dramatically affected the EC in both PNIPAM- and PAM-containing specimens. The addition of high-loading PEO (95 wt%) had a less detrimental effect on the EC, which was reduced to approximately half that of pristine PEDOT:PSS, as shown in Fig. 5(a). Additional experiments aimed to explore the correlation between the concentration of PEDOT:PSS nanoparticles in DI water and the EC of printed thin films. Fig. 5(b) demonstrated that as the concentration of PEDOT:PSS nanoparticles in the ink increased, the EC of the thin films also increased. This increase is likely due to the fact that a printed wet film with a higher concentration of PEDOT:PSS nanoparticles undergoes less water evaporation, resulting in a less porous and more conductive film.

The optimal concentration of 52 wt% PEO relative to PEDOT:PSS, which was found to enhance the EC in our previous study [33], was added to 1 wt%, 2.5 wt%, or 4.33 wt% PEDOT:PSS suspensions. These hybrid PEDOT:PSS-PEO inks were more electrically conducting than the pristine PEDOT:PSS ink, with the maximum conductivity reaching the conductivity value of ~ 17 S/cm. The results of the EC measurements presented in Fig. 5(a) cannot be directly compared to those in Fig. 5(b) because different brands of PEDOT:PSS were used (aqueous versus dry, respectively). The results reveal that printability of PEDOT:PSS redispersible particles in water can be significantly improved by adding PEO without compromising the EC, but rather enhancing it.

3.4. DIW fabrication of three-dimensional structures

In order to investigate the potential of PEO to enhance the printability of re-dispersible PEDOT:PSS suspension in the DIW process, this study involved the construction of three-dimensional structures, as detailed in section 2.2. Fig. 6(a) provides evidence that a 4.33 wt% PEDOT:PSS-52 wt% PEO suspension can be used to successfully create

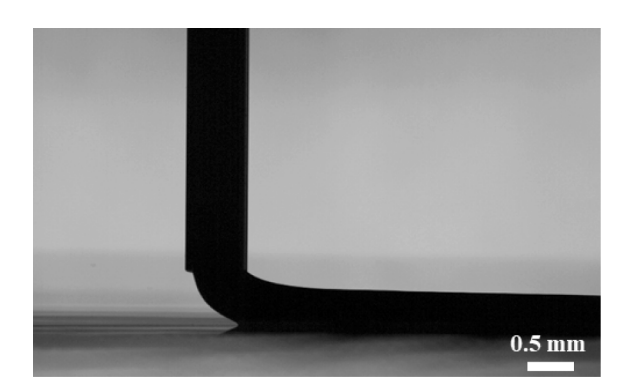


Fig. 4. Shape retention in DIW of re-dispersible PEDOT:PSS (4.33 wt% PEDOT: PSS with 52 wt% [when dried] PEO added) suspensions.

3D structures. In addition, the printed design unintentionally displayed a brim, which was thought to result from varying contact angles between the printed filaments and the substrates. To provide a comparison, the same structure was created using 4.33 wt% PEDOT:PSS without PEO, under the same experimental conditions, as shown in Fig. 6(b). However, one corner of the structure failed to adhere properly to the substrate and detached after only a few layers were printed. These results demonstrate the potential of PEO to enhance the printability of redispersible PEDOT:PSS aqueous suspension in the DIW process.

3.5. Electric-field-assisted direct ink writing of PEDOT:PSS-PEO inks

In previous work by this group [33], a threshold in the substrate translational speed was found when DIW printing. Even though this critical threshold of printing speed changes with the needle diameter, length, driving pressure and substrate chosen, it is easy to find it experimentally. This was done by repeatedly printing lines at increasing rates until failure due to the substrate moving too fast. These detrimental failures due to high-speed printing were suppressed using our eDIW process.

This study further evaluates eDIW performance using the modified 4.33 wt% PEDOT:PSS-52 wt% PEO suspension. It was printed at 0.5 m/s from a 22-gauge needle on a glass slide. It is important to note that 0.5 m/s is greater than the critical threshold with the results displayed in Fig. 7. Fig. 7(a) shows the filament printed by DIW without applying the electric field (the speed is different here compared to Fig. 6), whereas Fig. 7(b) is the filament printed with the electric field applied. In Fig. 7 (a) the printed filament is not even intact (i.e., a failed print), while the one displayed in Fig. 7(b) and printed with the electric field of 4.1 kV applied is not only intact, but also of good quality and resolution. These results unequivocally prove that eDIW is capable of printing 4.33 wt% PEDOT:PSS-52 wt% PEO suspension at a high speed and with a microscale resolution.

Additional experiments were conducted to assess the impact of even higher translational printing speeds on the quality and resolution of the deposited filaments in the presence of an electric field (i.e., eDIW). Fig. 8 (a) and 8(c) illustrate the changes in jet diameter (as observed in side views) with varying printing speeds, while Fig. 8(b) and 8(d) show the resulting deposited filaments (after drying) as seen from a top view, displaying the trace widths. The findings demonstrate that eDIW enables the production of controllable trace widths that are considerably smaller than the needle diameters. Additionally, Fig. 8 indicates that eDIW allows for the printing of high-quality traces at significantly high speeds, such as 8.64 m/s. Furthermore, the printing resolution improves with increasing printing speed, rather than decreasing. As illustrated in Fig. 8 (b) and 8(d), increasing the printing speed from 1.72 m/s to 8.64 m/s results in a decrease in trace width from 0.276 mm to 0.019 mm, despite using the same printing needle with a much larger inner diameter. Moreover, the 4.33 wt% PEDOT:PSS-52 wt% PEO suspension filaments deposited under such conditions can withstand all possible hydrodynamic instabilities, including drying-induced instabilities and corrugations. Following drying, the printed PEDOT:PSS-PEO traces remain intact, forming straight lines, much like those extruded.

3.6. High-humidity enhancement of the electrical conductivity

Similarly to the preceding sections, thin films were formed from traces of 4.33 wt% PEDOT:PSS-52 wt% PEO deposited in contact with each other using DIW at 30 mm/s. The resulting films were subjected to a high-humidity environment post-treatment to evaluate its effect on the EC. The findings, as shown in Fig. 9, indicate that the EC of the treated films could double after 4 h in a controlled-humidity chamber at relative humidity (RH) levels in the 80–90 % range. Note that at RH > 90 %, the result is inconclusive due to the large error bar.

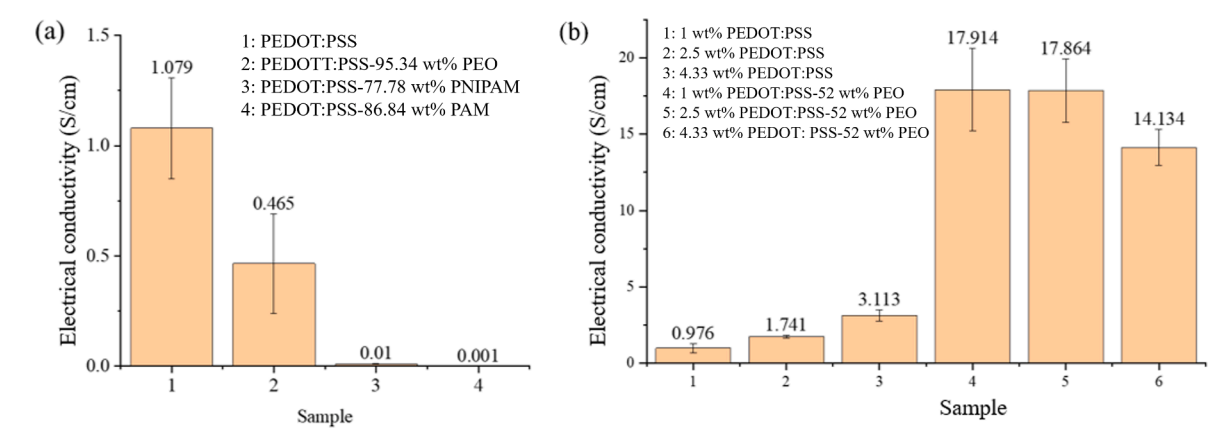


Fig. 5. The electrical conductivity of PEDOT:PSS-based inks. (a) Using additional dopant polymers (PEO, PNIPAM, PAM) as rheological modifiers. (b) Using redispersible PEDOT:PSS nanoparticles with added dopant PEO.

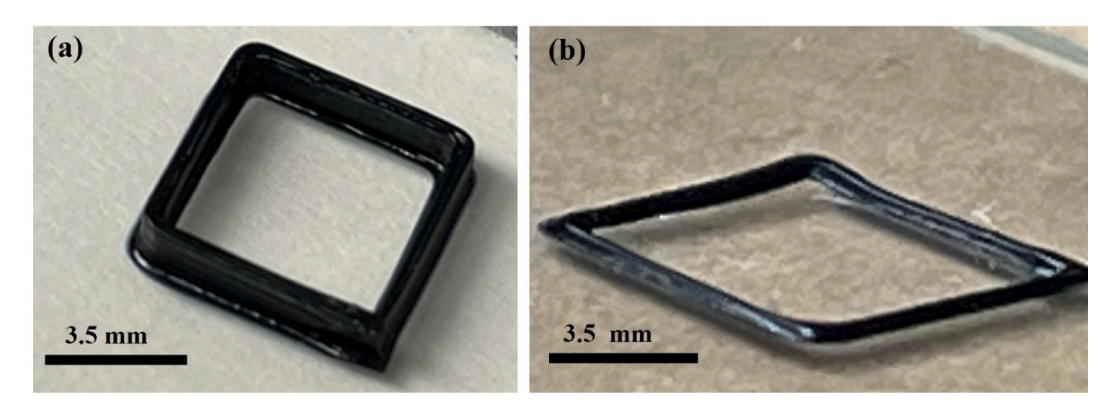


Fig. 6. DIW-formed 3D structures. (a) Optical image of the 3D structure printed using 4.33 wt% PEDOT:PSS-52 wt% PEO. (b) Optical image of the 3D structure printed using 4.33 wt% PEDOT:PSS: failed after printing a few layers.

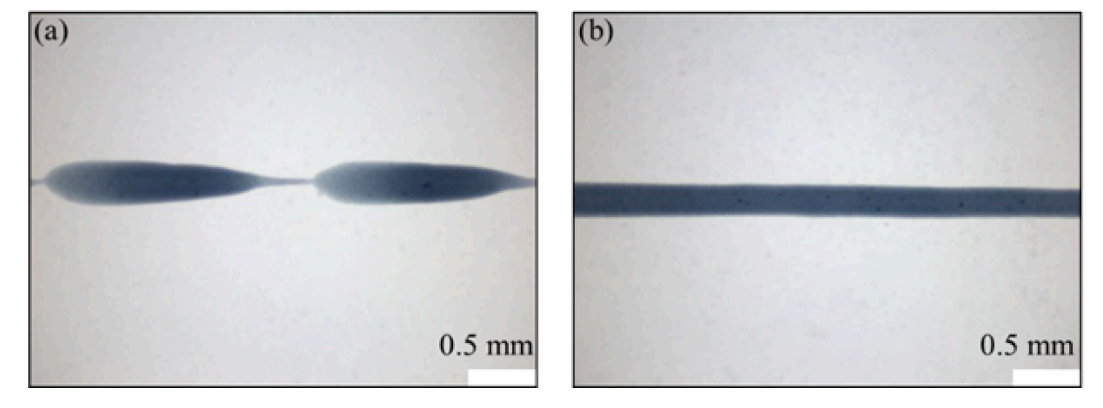


Fig. 7. eDIW printed filament versus the one printed without the electric field. (a) Microscope image of the print without applying the electric field. (b) Microscope image of the print with 4.1 KV applied to the governing electrode. The modified 4.33 wt% PEDOT:PSS-52 wt% PEO suspension was used.

For comparison, note that the electrical conductivity of mercury and molten sodium chloride are 104 S/cm (at room temperature) and 3.9 S/m (at 1173.15 $^{\circ}$ C), respectively, i.e., the printed PEDOT:PSS-PEO traces after high-humidity post-treatment reached about 50% of the electrical conductivity of mercury, and are 10 times more electrically-conducting than ionic liquids.

At the highest humidity level tested, RH=99%, the films became saturated with water droplets, which caused swelling and detachment. This phenomenon had a detrimental effect in two ways. First, the electrical conductivity could not be accurately measured, resulting in a large error bar at RH=99% in Fig. 9. Second, Fig. 10 shows the specimen before and after the 99% RH treatment, with clear evidence of

corrugations and cracks caused by the swelling of the film seen in Fig. 10 (b).

4. Conclusion and future work

4.1. Conclusion

Here, a novel type of high electrically conducting PEDOT:PSS-based ink was developed for fabrication of 2D, 2.5D and 3D structures using the direct ink writing (DIW) process. The optimal suspension of 4.33 wt % PEDOT:PSS-52 wt% PEO established here not only possesses the electrical conductivity > 15 times that of the electrical conductivity of

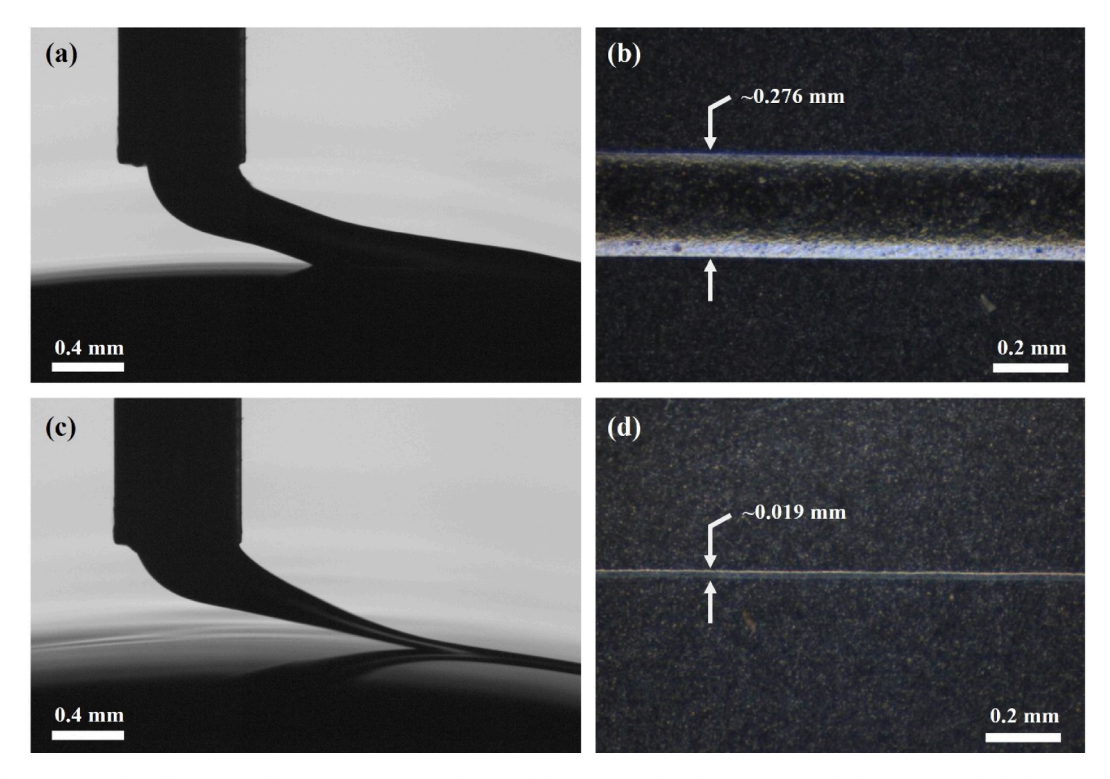


Fig. 8. Effect of printing speed on filament resolution in eDIW. (a) Side view of the jet printed at the printing speed of 1.72 m/s, and (b) the corresponding top view of the deposited dried filament on a glass slide, with a trace width of 0.276 mm. (c) Side view of the jet printed at the printing speed of 8.64 m/s, and (d) the corresponding top view of the deposited dried filament on a glass slide, with a trace width of 0.019 mm, almost invisible by the naked eye. The modified 4.33 wt% PEDOT:PSS-52 wt% PEO suspension was used, and the applied voltage was 4.1 kV.

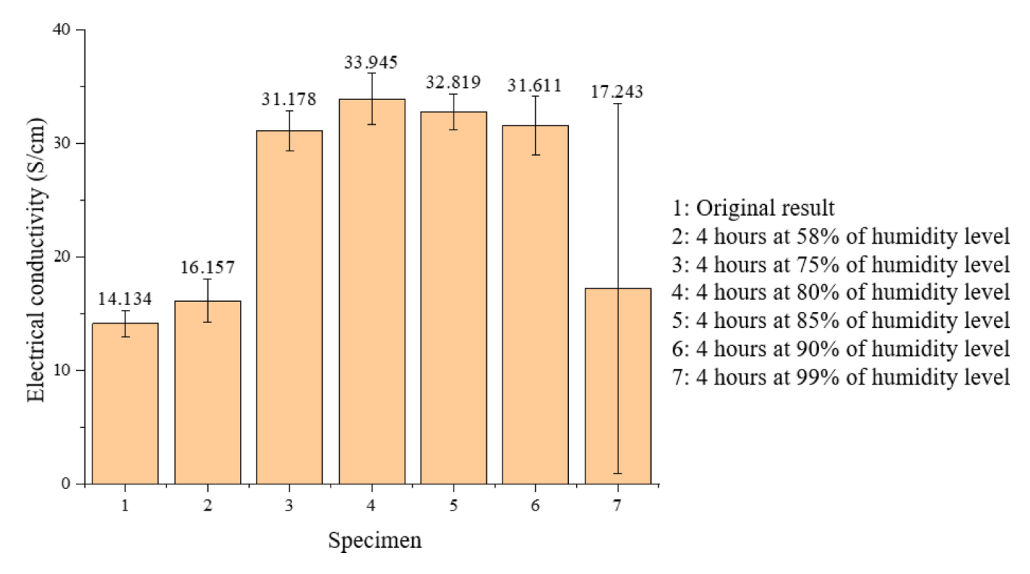


Fig. 9. The electrical conductivity of 4.33 wt% PEDOT:PSS-52 wt% PEO DIW-printed films after storage for 4 h at different relative humidity levels.

pristine PEDOT:PSS, but after a post-treatment in a humidity-controlled chamber (at 80–90% relative humidity for 4 h) can double its conductivity compared to the pre-treatment one of Ref. [33]. Specifically, films formed by means of DIW of 4.33 wt% PEDOT:PSS-52 wt% PEO after such a post-treatment can reach 50% of the electrical conductivity of mercury and ten-fold that of ionic liquids. It is also shown that the other two secondary dopants explored here except PEO (PNIPAM, and PAM) significantly diminish the electrical conductivity, and thus should be avoided. Moreover, it was demonstrated here that the optimal suspension of 4.33 wt% PEDOT:PSS-52 wt% PEO possesses a highly favorable combination of the shear, elongational, and thixotropic rheological

properties (the latter were explored here for the first time) and thus, reveals an excellent printability and filament-shape retention after printing.

In addition, it was demonstrated that our novel electrostatically-assisted direct ink writing (eDIW) can print this material at extremely fast speeds, of $\sim 9~\text{m/s}$, which is one to three orders of magnitude faster than the current commercial 3D printers. The optimal suspension of 4.33 wt% PEDOT:PSS-52 wt% PEO was used to create 2D, 2.5D and 3D functional structures for the first time. Moreover, it was demonstrated that in eDIW the printing resolution increases with the printing speed, rather than decreases. In particular, the trace width of 0.019 mm was





Fig. 10. Images of 4.33 wt% PEDOT:PSS-52 wt% PEO film. (a) Original printed film. (b) After storage at RH = 99% for 4 h.

observed after DIW at \sim 9 m/s.

4.2. Future work

The present results point at several fundamental physical and applied scientific questions to be addressed in future in relation to the novel eDIW process and a new conducting ink, 4.33 wt% PEDOT:PSS-52 wt% PEO suspension and traces formed from it:

- (i). Does the electrode configuration in eDIW generate a Coulomb force that pulls the extruded polymer PEDOT:PSS-PEO ink in the direction of printing, allowing faster substrate translation speed, thinner and narrower filament, and successful deposition on rough surfaces? A good starting point to address these questions would be our previous work [33].
- (ii). Do the extrusion pulling and high translation speed create a highenough shear force, resulting in a phase-segregated morphology of the printed polymer composite and an enhanced in-plane electrical conductivity? Some relevant useful theoretical ideas in this respect could be found in Refs. [48,49].
- (iii). What is the physical mechanism responsible for a significant increase in the DIW-printed PEDOT:PSS-PEO films post-treated at high relative humidity? Here the starting points could be the atomistic and DFT simulations of the type of Refs. [50,51].

Research directions and approaches outlined in the present work aim to engage new collaborations between eDIW in disciplines ranging from thin films to complex freeform structures. The use of conducting polymer inks (specifically, PEDOT:PSS-PEO) is practically unexplored in the DIW-related literature. Understanding how the other polymer additives (secondary dopants) influence the DIW printability and the electrical conductivity of printed traces provides new tools that promote rapid functionality increase within a technological domain, which holds great promise. Moreover, such interface-science related phenomena could stimulate a deeper insight into suspensions of nanoscale PEDOT:PSS particles and span the macroscopic (rheological and electrohydrodynamic) level with the atomistic level (the conductive band in conducting polymers, polarons, bipolarons and charge-transport mechanisms in conducting polymers [52,53]).

$CRediT\ authorship\ contribution\ statement$

J. Plog: Methodology, Investigation, Data curation, Writing -

original draft. **X. Wang:** Methodology, Investigation, Data curation, Writing – original draft. **K.M. Lichade:** Investigation. **Y. Pan:** Conceptualization, Methodology, Supervision, Writing – review & editing, Funding acquisition. **A.L. Yarin:** Conceptualization, Methodology, Supervision, Writing – review & editing, Funding acquisition.

Declaration of Competing Interest

The authors declare that they have no known competing financial interests or personal relationships that could have appeared to influence the work reported in this paper.

Data availability

Data will be made available on request.

Acknowledgment

This project was partially supported by National Science Foundation (NSF) Grants 1825626 and 2224749.

References

- M. Borghetti, M. Serpelloni, E. Sardini, S. Pandini, Mechanical behavior of strain sensors based on PEDOT: PSS and silver nanoparticles inks deposited on polymer substrate by inkjet printing, Sens. Actuators, A 243 (2016) 71–80.
- [2] S. Nambiar, J.T.W. Yeow, Conductive polymer-based sensors for biomedical applications, Biosens. Bioelectron. 26 (5) (2011) 1825–1832.
- [3] S.L. Lee, C.J. Chang, Recent developments about conductive polymer based composite photocatalysts, Polymers 11 (2019) 206.
- [4] H. Deng, L. Lin, M. Ji, S. Zhang, M. Yang, Q. Fu, Progress on the morphological control of conductive network in conductive polymer composites and the use as electroactive multifunctional materials, Prog. Polym. Sci. 39 (4) (2014) 627–655.
 [5] H. Shirakawa, E.J. Louis, A.G. MacDiarmid, C.K. Chiang, A.J. Heeger, Synthesis of
- [5] H. Shirakawa, E.J. Louis, A.G. MacDiarmid, C.K. Chiang, A.J. Heeger, Synthesis of electrically conducting organic polymers: Halogen derivatives of polyacetylene, (CH)x Journal of the Chemical Society, Chem. Commun. 16 (1977) 578–580.
- [6] Y.W. Park, A.J. Heeger, M.A. Druy, A.G. MacDiarmid, Electrical transport in doped polyacetylene, J. Chem. Phys. 73 (1980) 946–957.
- [7] Y.W. Park, C. Park, Y.S. Lee, C.O. Yoon, H. Shirakawa, Y. Suezaki, K. Akagi, Electrical conductivity of highly-oriented-polyacetylene, Solid State Commun. 65 (2) (1988) 147–150.
- [8] R. Cherrington, J. Liang, Materials and deposition processes for multifunctionality. Design and manufacture of plastic components for multifunctionality: Structural composites, injection molding, and 3D printing, (2016) 19-21.
- [9] J.C. Chien. Polyacetylene: Chemistry, Physics, and Material Science, Elsevier, 2012.
- [10] E.M. Geniès, A. Boyle, M. Lapkowski, C. Tsintavis, Polyaniline: A historical survey, Synth. Met. 36 (2) (1990) 139–182.

- [11] H.-A. Ho, M. Boissinot, M.G. Bergeron, G. Corbeil, K. Doré, D. Boudreau, M. Leclerc, Colorimetric and fluorometric detection of nucleic acids using cationic polythiophene derivatives, Angew. Chem. 114 (9) (2002) 1618–1621.
- [12] X. Crispin, F.L.E. Jakobsson, A. Crispin, P.C.M. Grim, P. Andersson, A. Volodin, C. van Haesendonck, M. van der Auweraer, W.R. Salaneck, M. Berggren, The origin of the high conductivity of poly (3, 4-ethylenedioxythiophene) poly (styrenesulfonate) (PEDOT PSS) plastic electrodes, Chem. Mater. 18 (18) (2006) 4354–4360.
- [13] X. Lan, C. Liu, T. Wang, J. Hou, J. Xu, R. Tan, G. Nie, F. Jiang, Effect of functional groups on the thermoelectric performance of carbon nanotubes, J. Electron. Mater. 48 (11) (2019) 6978–6984.
- [14] J. Zhang, W. Ding, Z. Zhang, J. Xu, Y. Wen, Preparation of black phosphorus-PEDOT: PSS hybrid semiconductor composites with good film-forming properties and environmental stability in water containing oxygen, RSC Adv. 6 (80) (2016) 76174–76182.
- [15] W. Yan, J. Li, G. Zhang, L. Wang, D. Ho, A synergistic self-assembled 3D PEDOT: PSS/graphene composite sponge for stretchable microsupercapacitors, J. Mater. Chem. A 8 (2) (2020) 554–564.
- [16] T. Takano, H. Masunaga, A. Fujiwara, H. Okuzaki, T. Sasaki, PEDOT nanocrystal in highly conductive PEDOT: PSS polymer films, Macromolecules 45 (9) (2012) 3850-3865
- [17] A.M. Nardes, M. Kemerink, R.A.J. Janssen, Anisotropic hopping conduction in spin-coated PEDOT: PSS thin films, Phys. Rev. B 76 (2007) 085208.
- [18] Y. Ding, J. Yang, C.R. Tolle, Z. Zhu, Flexible and compressible PEDOT: PSS@ melamine conductive sponge prepared via one-step dip coating as piezoresistive pressure sensor for human motion detection, ACS Appl. Mater. Interfaces 10 (18) (2018) 16077–16086.
- [19] S.H. Eom, S. Senthilarasu, P. Uthirakumar, S.C. Yoon, J. Lim, C. Lee, H.S. Lim, J. Lee, S.-H. Lee, Polymer solar cells based on inkjet-printed PEDOT: PSS layer, Org. Electron. 10 (3) (2009) 536–542.
- [20] S. Kumar, M. Umar, A. Saifi, S. Kumar, S. Augustine, S. Srivastava, B.D. Malhotra, Electrochemical paper based cancer biosensor using iron oxide nanoparticles decorated PEDOT: PSS, Anal. Chim. Acta 1056 (2019) 135–145.
- [21] Z. Zhu, T. Mankowski, K. Balakrishnan, A.S. Shikoh, F. Touati, M.A. Benammar, M. Mansuripur, C.M. Falco, Ultrahigh aspect ratio copper-nanowire-based hybrid transparent conductive electrodes with PEDOT: PSS and reduced graphene oxide exhibiting reduced surface roughness and improved stability, ACS Appl. Mater. Interfaces 7 (30) (2015) 16223–16230.
- [22] N. Abdullayeva, M. Sankir, Influence of electrical and ionic conductivities of organic electronic ion pump on acetylcholine exchange performance, Materials 10 (2017) 586.
- [23] F. Zhao, X. Chen, Z. Yi, F. Qin, Y. Tang, W. Yao, Z. Zhou, Y. Yi, Study on the solar energy absorption of hybrid solar cells with trapezoid-pyramidal structure based PEDOT: PSS/c-Ge, Sol. Energy 204 (2020) 635–643.
- [24] Y. Sun, J. Zheng, Y. Yang, J. Zhao, J. Rong, H. Li, L. Niu, Design advanced porous Polyaniline-PEDOT: PSS composite as high performance cathode for sodium ion batteries, Compos. Commun. 24 (2021) 100674.
- [25] J.A. Lewis, Direct ink writing of 3D functional materials, Adv. Funct. Mater. 16 (17) (2006) 2193–2204.
- [26] L. del-Mazo-Barbara, M.-P. Ginebra, Rheological characterisation of ceramic inks for 3D direct ink writing: A review, J. Eur. Ceram. Soc. 41 (16) (2021) 18–33.
- [27] Y. Jiang, X. Wang, J. Plog, A.L. Yarin, Y. Pan, Electrowetting-assisted direct ink writing for low-viscosity liquids, J. Manuf. Process. 69 (2021) 173–180.
- [28] H. Yuk, B. Lu, S. Lin, K. Qu, J. Xu, J. Luo, X. Zhao, 3D printing of conducting polymers, Nat. Commun. 11 (2020) 1–8.
- [29] J.Y. Kim, J.H. Jung, D.E. Lee, J. Joo, Enhancement of electrical conductivity of poly (3, 4-ethylenedioxythiophene)/poly (4-styrenesulfonate) by a change of solvents, Synth. Met. 126 (2-3) (2002) 311–316.
- [30] J. Ouyang, Y. Yang, Conducting polymer as transparent electric glue, Adv. Mater. 18 (16) (2006) 2141–2144.
- [31] A. Onorato, M.A. Invernale, I.D. Berghorn, C. Pavlik, G.A. Sotzing, M.B. Smith, Enhanced conductivity in sorbitol-treated PEDOT–PSS. Observation of an in situ cyclodehydration reaction, Synth. Met. 160 (21-22) (2010) 2284–2289.

- [32] S.L. Lai, M.Y. Chan, M.K. Fung, C.S. Lee, S.T. Lee, Concentration effect of glycerol on the conductivity of PEDOT film and the device performance, Mater. Sci. Eng. B 104 (1-2) (2003) 26–30.
- [33] X. Wang, J. Plog, K. Lichade, A.L. Yarin, Y. Pan, 3D printing of highly conductive PEDOT: PSS-based polymers, J. Manuf. Sci. Eng. 145 (2023) 011008.
- [34] J. Plog, Y. Jiang, Y. Pan, A.L. Yarin, Electrostatically-assisted direct ink writing for additive manufacturing, Addit. Manuf. 39 (2021) 101644.
- [35] M. Chen, L. Yang, Y. Zheng, Y. Huang, L. Li, P. Zhao, S. Wang, L. Lu, X. Cheng, Yield stress and thixotropy control of 3D-printed calcium sulfoaluminate cement composites with metakaolin related to structural build-up, Constr. Build. Mater. 252 (2020) 119090.
- [36] A.L. Yarin, B. Pourdeyhimi, S. Ramakrishna. Fundamentals and Applications of Micro- and Nanofibers, Cambridge University Press, Cambridge, 2014.
- [37] J. Plog, J. Wu, Y.J. Dias, F. Mashayek, L.F. Cooper, A.L. Yarin, Reopening dentistry after COVID-19: Complete suppression of aerosolization in dental procedures by viscoelastic Medusa Gorgo, Phys. Fluids 32 (8) (2020) 083111.
- [38] M. Stelter, G. Brenn, A.L. Yarin, R.P. Singh, F. Durst, Validation and application of a novel elongational device for polymer solutions, J. Rheol. 44 (3) (2000) 595–616.
- [39] M. Stelter, G. Brenn, A.L. Yarin, R.P. Singh, F. Durst, Investigation of the elongational behavior of polymer solutions by means of an elongational rheometer, J. Rheol. 46 (2) (2002) 507–527.
- [40] A.L. Yarin, E. Zussman, A. Theron, S. Rahimi, Z. Sobe, D. Hasan, Elongational behavior of gelled propellant simulants, J. Rheol. 48 (1) (2004) 101–116.
- [41] E. Zussman, A.L. Yarin, R.M. Nagler, Age-and flow-dependency of salivary viscoelasticity, J. Dent. Res. 86 (3) (2007) 281–285.
- [42] F.M. Smits, Measurement of sheet resistivities with the four-point probe, Bell Syst. Tech. J. 37 (1958) 711–718.
- [43] J. Plog, X. Wang, Y. Pan, A.L. Yarin, Electrostatically-assisted direct ink writing with superior speed and resolution, J. Manuf. Process. 76 (2022) 752–757.
- [44] C. Yi, A. Wilhite, L. Zhang, R. Hu, S.S.C. Chuang, J. Zheng, X. Gong, Enhanced thermoelectric properties of polymer poly(3,4-ethylenedioxythiophene):poly (styrenesulfonate) by binary secondary dopants, ACS Appl. Mater. Interfaces 7 (2015) 8984–8989.
- [45] K. Jain, A.Y. Mechandziyski, I. Zozoulenko, L. Wagberg, PEDOT:PSS nano-particles in aqueous media: A comparative experimental and molecular dynamics study of particle size, morphology and z-potential, J. Colloid Interface Sci. 584 (2021) 57–66.
- [46] K. Fu, R. Lv, B. Na, S. Zou, R. Zeng, B. Wang, H. Liu, Mixed ion-electron conducting PEO/PEDOT: PSS miscible blends with intense electrochromic response, Polymer 184 (2019) 121900.
- [47] M. Jia, J. Zhang, Thermoresponsive PEDOT: PSS/PNIPAM conductive hydrogels as wearable resistive sensors for breathing pattern detection, Polym. J. 54 (6) (2022) 793–801.
- [48] M.N. Gueye, A. Carella, J. Faure-Vincent, R. Demadrille, J.-P. Simonato, Progress in understanding structure and transport properties of PEDOT-based materials: A critical review, Prog. Mater Sci. 108 (2020) 100616.
- [49] H. Shi. Optimizing the thermoelectric performance of PEDOTs. Chapter 5 in Advanced PEDOT Thermoelectric Materials, Elsevier, Amsterdam, 2022, pp. 119–143.
- [50] H. Makki, A. Troisi, Morphology of conducting polymer blends at the interface of conducting and insulating phases: Insight from PEDOT:PSS atomistic simulations, J. Mater. Chem. C 10 (42) (2022) 16126–16137.
- [51] V. Yurkiv, J. Wu, S. Halder, R. Granda, A. Sankaran, A.L. Yarin, F. Mashayek, Water interaction with dielectric surface: A combined ab-initio modeling and experimental study, Phys. Fluids 33 (4) (2021) 042012.
- [52] S.D. Kang, G.J. Snyder, Charge-transport model for conducting polymers, Nature Mat. 16 (2) (2017) 252–257.
- [53] S.A. Gregory, R. Hanus, A. Atassi, J.M. Rinehart, J.P. Wooding, A.K. Menon, M. D. Losego, G.J. Snyder, S.K. Yee, Quantifying charge carrier localization in chemically doped semiconducting polymers, Nature Mat. 20 (2021) 1414–1423.